XX Polish Fluid Mechanics Conference,
Gliwice, 17-20 September 2012

THE INFLUENCE OF WIND STRUCTURE AND ASPECT RATIO OF CIRCULAR CYLINDERS ON MEAN WIND PRESSURE COEFFICIENT

Tomasz LIPECKI[1], Paulina JAMIŃSKA[2],
1Lublin University of Technology, Lublin, Poland;
2Lublin University of Technology, Lublin, Poland;
E-mail: p.jaminska@pollub.pl, t.lipecki@pollub.pl

Abstract: The paper presents analyses of the mean wind pressure coefficient distribution on the surfaces of circular cylinders. The experiment was performed in a boundary layer wind tunnel in the Wind Engineering Laboratory in Cracow, Poland. Three models were examined in the wind tunnel. The influence of the aspect ratio and wind parameters (mean wind speed profile, turbulence intensity profile, power spectral density functions) on the mean wind pressure coefficient distribution and its standard deviation was considered during the tests.

Key words: wind tunnel, mean wind pressure coefficient, circular cylinder, wind structure, aspect ratio

INTRODUCTION

Cylinders of circular cross-sections were investigated in wind tunnels by many researches. Experiments were carried out in order to obtain pressure distributions on the surface, the lift and drag force coefficients, Strouhal number, the correlation coefficient of the load, vortex excitation parameters, etc. Most of the tests were carried out with the Reynolds number (Re) in the subcritical range, on smooth models, in case of the 2D flow. Recent studies have increasingly been focused on the influence of the roughness of the cylinder surface and on the influence of flow turbulence on the behavior of the tested model, as well as on the 3D flow around the free-end of the model. Some recent studies on stationary rigid cylinders with free-end are summarized below.

Uematsu and Yamada (1995, 1995b) performed measurements of rms pressure coefficient on cantilever model of the cylinder (H/D = 1-5, H – height, D – diameter), at unsteady flow. The authors gave an empirical equation describing changes of Strouhal number (St) with changes of aspect ratio H/D and the cylinder surface roughness. The effect of aspect ratio (H/D = 1.71 - 8.5) on the lift force was described by Garg and Niemann (1995) and Garg et al. (1999). Pressure distributions in different cross-sections were used to calculate the forces operating on the model and their coefficients and cross correlations. They also proposed the relationship of Strouhal number in the function of the distance from the top of the cylinder. Lee and Park (1999) and Park and Lee (2000) studied the effect of aspect ratio (H/D = 6.1 10, 13, 17.3) and the free-end of the cantilever cylinder on vortex excitation parameters. The authors measured power spectral densities of vortex excitation for different ratios H/D, the cross-correlation functions of velocities in two points lying on opposite sides of the model cross-section. They also presented distributions of pressure coefficient. In the next work by Park and Lee (2002) the flow around the free-end in different cases of boundary layer was investigated. Park and Lee (2004) developed previous studies taking into account shape modifications of the model free-end. In both papers detailed visualization of the flow was presented. Luo et al. (1996) studied the cylinder model with the free-end (H/D = 4, 6, 8) in the steady flow. On the basis of pressure measurements along the height, it was found that the

flow around the free-end was in the interaction with the flow shedding from both sides of the upper half of the cylinder. This effect for cylinders with a relatively large aspect ratio H/D introduces disturbances in the formation of vortices and causes the lack of the clear Strouhal frequency near the free-end. Sumner and Heseltine (2004) and Sumner et al. (2004) investigated the vortices forming near the free-end of the cylinder (H/D = 3, 5, 7, 9), at $Re = 6 \cdot 10^4$. Velocity fields in the excitation area were measured and averaged in time, and then strength of vortices in every measuring point were estimated. General conclusion was that the vortex excitation for the model with the free-end occurs only in certain areas along the height of the model (cf. Garg et al., 1995, Garg et al., 1999). In the next paper by Sumner and Heseltine (2008) detailed information about the tip vortices structure and its streamwise development were provided. The turbulent wake of cylinders was investigated experimentally, at $Re = 6 \cdot 10^4$ by Adaramola et al. (2006) (c.f. Sumner and Heseltine 2004, 2008, Sumner et al. 2004). The turbulent wake structure was similar for cylinders of aspect ratios of 5, 7, 9 whereas distinctly different for the cylinder of aspect ratio of 3. More details about the flow around the model of aspect ratio of 9 are presented in the paper by Adaramola et al. (2010). Capone and Lauchle (2000) developed semi-empirical models for determining the drag and lift forces acting on the cylinder of the finite length (H/D = 2). These models consist of a description of the spatial changes in values of rms pressure and correlation length along the span. The authors in the next paper Capone and Lauchle (2002) extended the semi-empirical model of the 3D flow around the free-end of the cylinder. Cao et al. (2007) studied experimentally whereas Cao and Tamura (2008) studied experimentally and numerically the flow around cylinders (H/D = 2.22, 4, 8) in linear shear flows, at $Re = 1.7 \cdot 10^4$-$3.6 \cdot 10^4$. Vortex shedding was investigated by examination of Strouhal number and base pressure variations with respect to shear parameter. Also the mean pressure distributions around cylinder as well as drag and lift forces were considered in these studies. The 3D effect of the flow passing over the free-end on vortex shedding in case of the cylinder of small aspect ratio of 3, at $Re = 6 \cdot 10^4$ - $11 \cdot 10^4$ was investigated by Iungo et al. (2012). Pressures, forces and velocities measurements were conducted during these tests.

RESEARCH DESCRIPTION

Models

Experiments were performed in the boundary layer wind tunnel of the Wind Engineering Laboratory in Cracow, Poland. The basic dimensions of the working section of the close circuit wind tunnel are: width – 2.20 m, height – 1.4-1.6 m, length – 10 m. Three rigid models of circular cross-sections were investigated. Basic dimension of models are collected in Table 1, where H – height, D – diameter, λ – aspect ratio. Each model was placed vertically on the rotational table in the center of the working section (Fig. 1).

Table 1. Models characteristics.

Model	H	D	λ
	[m]	[m]	[-]
C1	100	20	5
C2	99	11	9
C3	100	5	20

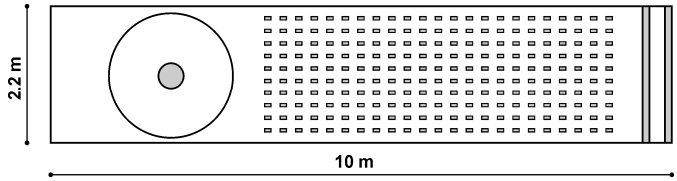

Figure 1. Working section of the wind tunnel with the model placed on the rotational table.

Wind parameters

A mean wind speed profile is formed in the first part of the working section of the wind tunnel at the distance of 6 m. Respective wind profiles are obtained by using various barriers, spires and blocks. The blockage is reduced by slotted side walls.

Detailed measurements allowed to select six different wind structures characterized by mean wind speed profile, turbulence intensity profile and power spectral density functions for which further tests were conducted (Fig. 2). The following relations were applied for wind speed profile, turbulence intensity profile and PSD function:

$$v(z) = k \cdot z^{\alpha} \quad \text{for} \quad z > z_{min} \qquad I_v(z) = \frac{\sigma(z)}{\bar{v}(z)} \qquad G(f) = \frac{bf^2}{\left(1 + cf^2\right)^d} \tag{1}$$

where: z – height [cm], z_{min} – minimum height [cm] for which all profiles have the same value at 70 cm, k and α – values selected by the least squares method, $\bar{v}(z)$ – mean wind speed, $\sigma(z)$ – standard deviation of wind speed, b, c, d –coefficients selected by the least squares method. Respective plots are collected in Figure 2.

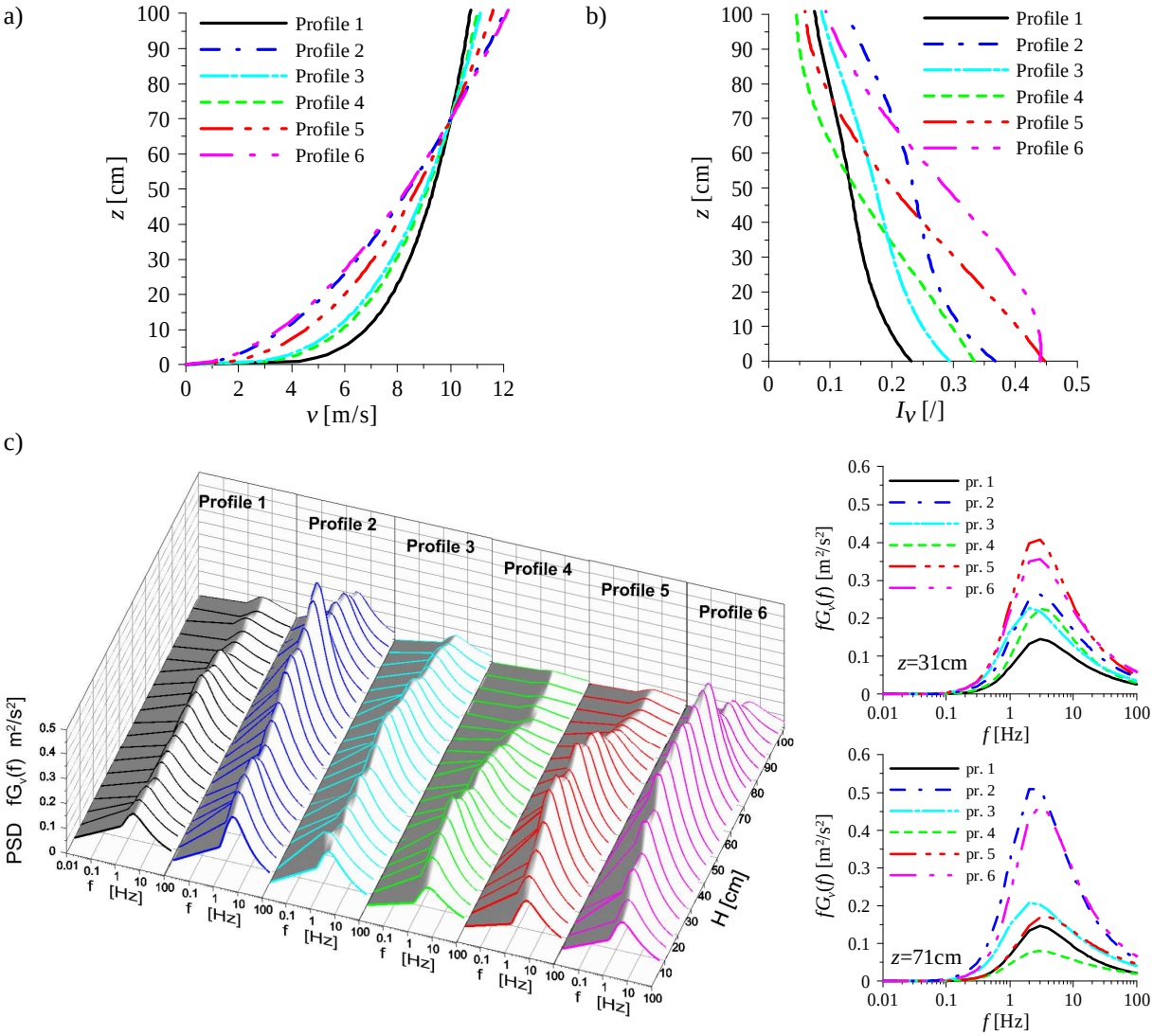

Figure 2. Wind characteristics: a) profiles of the mean wind speed, b) profiles of the intensity of turbulence, c) PSD functions: the spatial distributions and examples at two levels.

Experiment parameters

Tests were focused on measurements of mean wind pressure on the surface of the model.

Pressure points were located on 16 circumferences in 6 vertical sections (Fig. 3). The rotation of the model in the angle range 0°-60° with 5° step was applied. Top covers were also equipped with pressure taps in order to investigate 3D character of the flow. Data were obtained for the whole circumference (0°-360°) in cases of models C1 and C2, and for half of the circumference (0°-180°) in case of model C3.

Mean pressure was obtained in each point of the model from dynamic pressure measurements. The mean pressure was normalized by reference pressure which was measured in the right front of the model at the height of 70 cm. The data from pressure taps was archiving with 500 Hz frequency in the time range of 30 sec, which gave 6000 probes. The measuring scheme is presented in Figure 4. The mean wind static pressure coefficient C_p and its standard deviation σ_p were calculated using the following equations:

$$C_p = p / \left(0.5 \cdot \rho \cdot v_0^2\right), \qquad \sigma_p = \sigma / \left(0.5 \cdot \rho \cdot v_0^2\right) \tag{2}$$

where: p – mean dynamic pressure in the given point of the model, σ_p – standard deviation of the dynamic pressure, ρ – air density, v_0 – wind speed in undisturbed flow in the reference point, at the front of the structure, at height z = 70 cm.

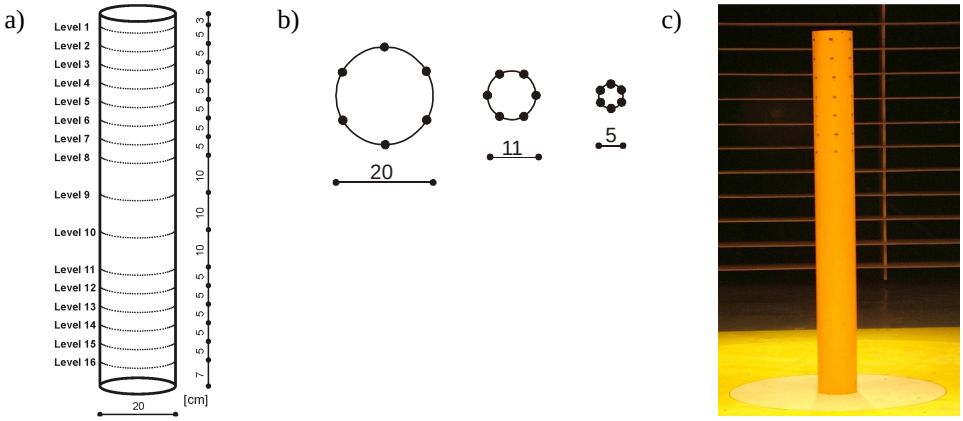

Figure 3. Experimental set-up: a) distribution of pressure points along the height, b) distribution of pressure points around the circumference, c) model C1 in the wind tunnel.

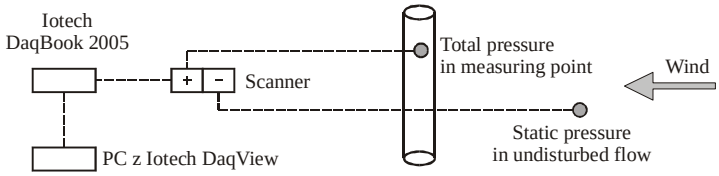

Figure 4. Measuring scheme.

RESULTS

The mean wind pressure coefficient C_p and its standard deviation σ_p are presented for three models. There are three sets of plots concerning changes in the value of C_p and σ_p: overall changes at surface plots (Fig. 5), circumferential changes (Fig. 6), vertical changes (Fig. 7).

Surface distribution

Surface plots were made for each case of the approaching flow. The same settings for limits of C_p and σ_p values on spatial plots are kept in Figure 5 (max = 3, min = -6 for C_p and max = 1.7, min = 0 for σ_p) according to the enclosed legend.

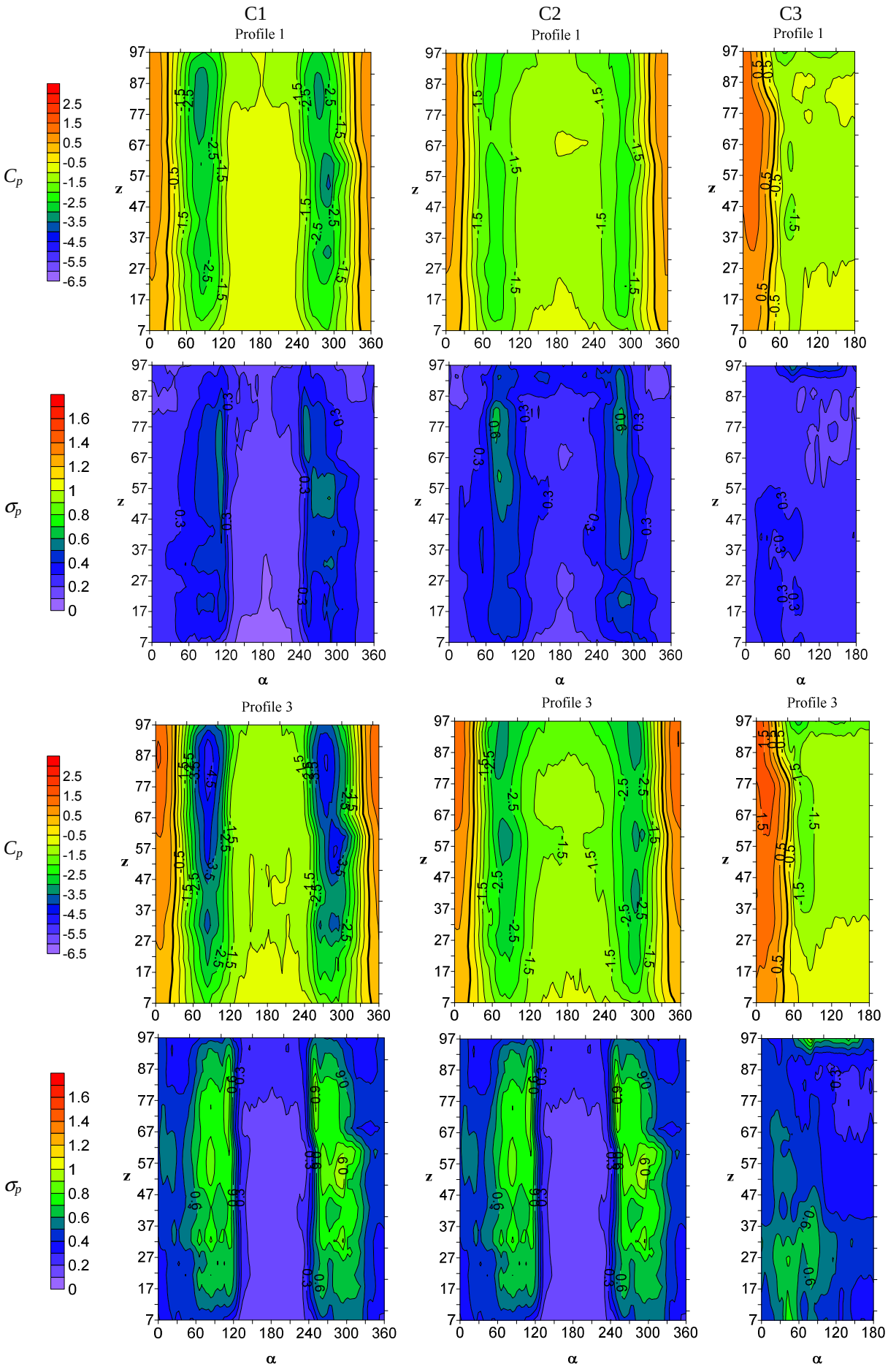
C1
C2
C3
Profile 1
Profile 1
Profile 1
Profile 3
Profile 3
Profile 3
C_p
σ_p
C_p
σ_p
2.5
1.5
0.5
-0.5
-1.5
-2.5
-3.5
-4.5
-5.5
-6.5
1.6
1.4
1.2
1
0.8
0.6
0.4
0.2
0
z
α
0
60
120
180
240
300
360
7
17
27
37
47
57
67
77
87
97

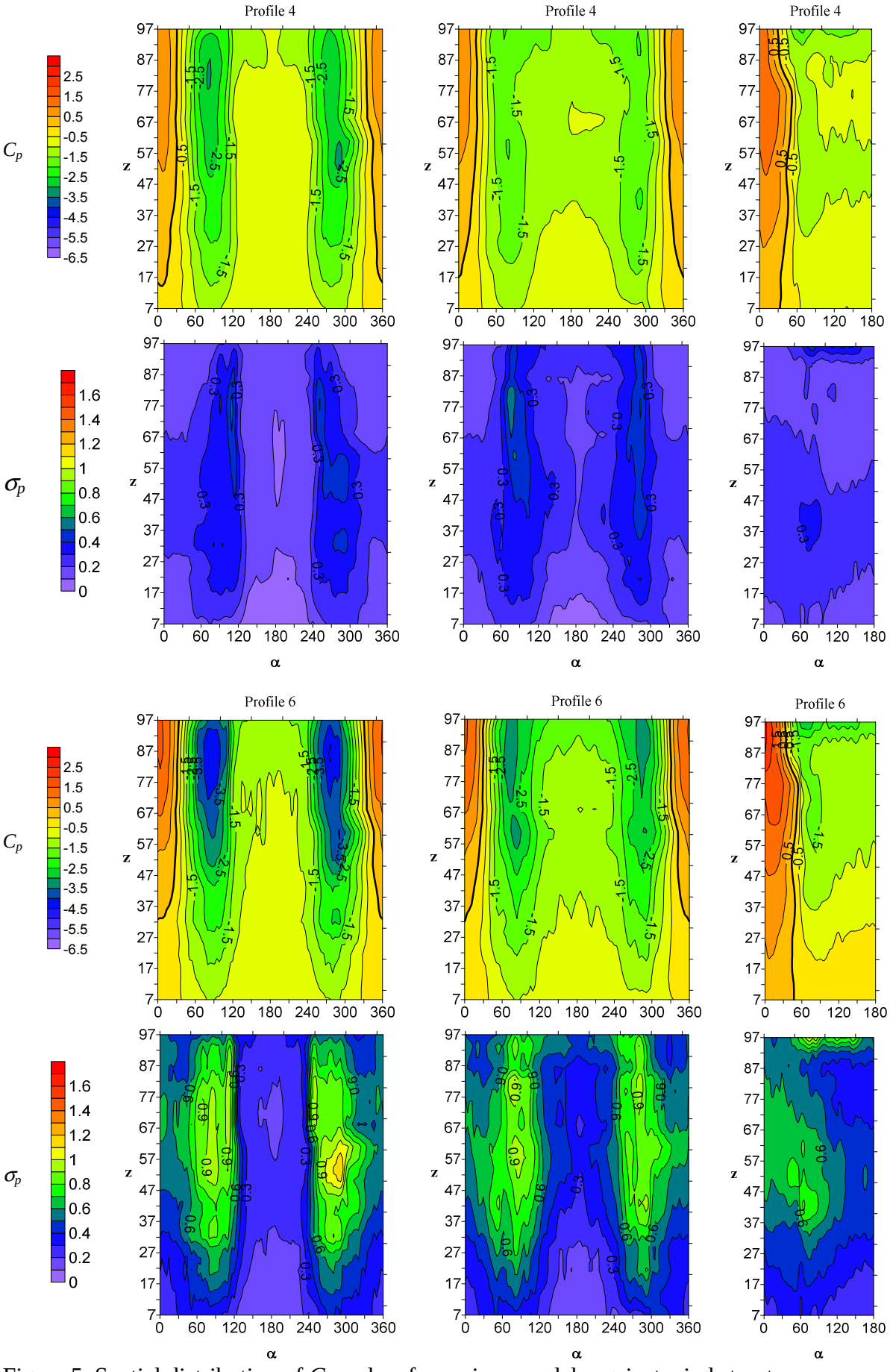

Figure 5. Spatial distribution of C_p and σ_p for various models against wind structure.

Circumferential distribution

Circumferential distributions of the mean wind pressure coefficient and its standard deviation are presented for chosen levels distributed along the height of models – near the top and the base and in the middle (level 1 – 97 cm, level 2 – 92 cm, level 7 – 67 cm, level 8 – 62 cm, level 15 – 12 cm, level 16 – 7 cm) in six cases of the approaching flow. The same colors, as for profiles in Figure 2, were applied in Figures 6 and 7 according to the enclosed legend.

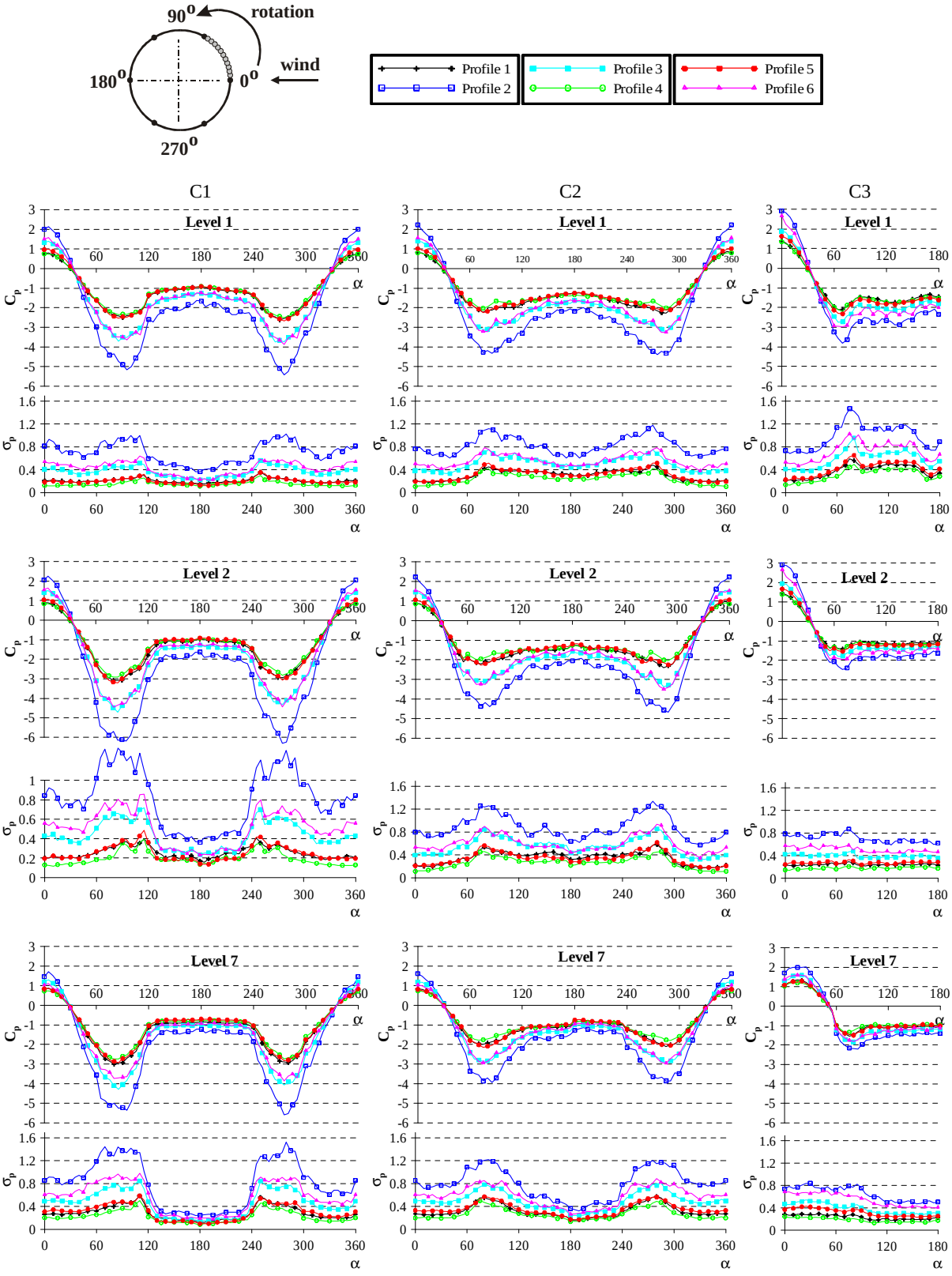

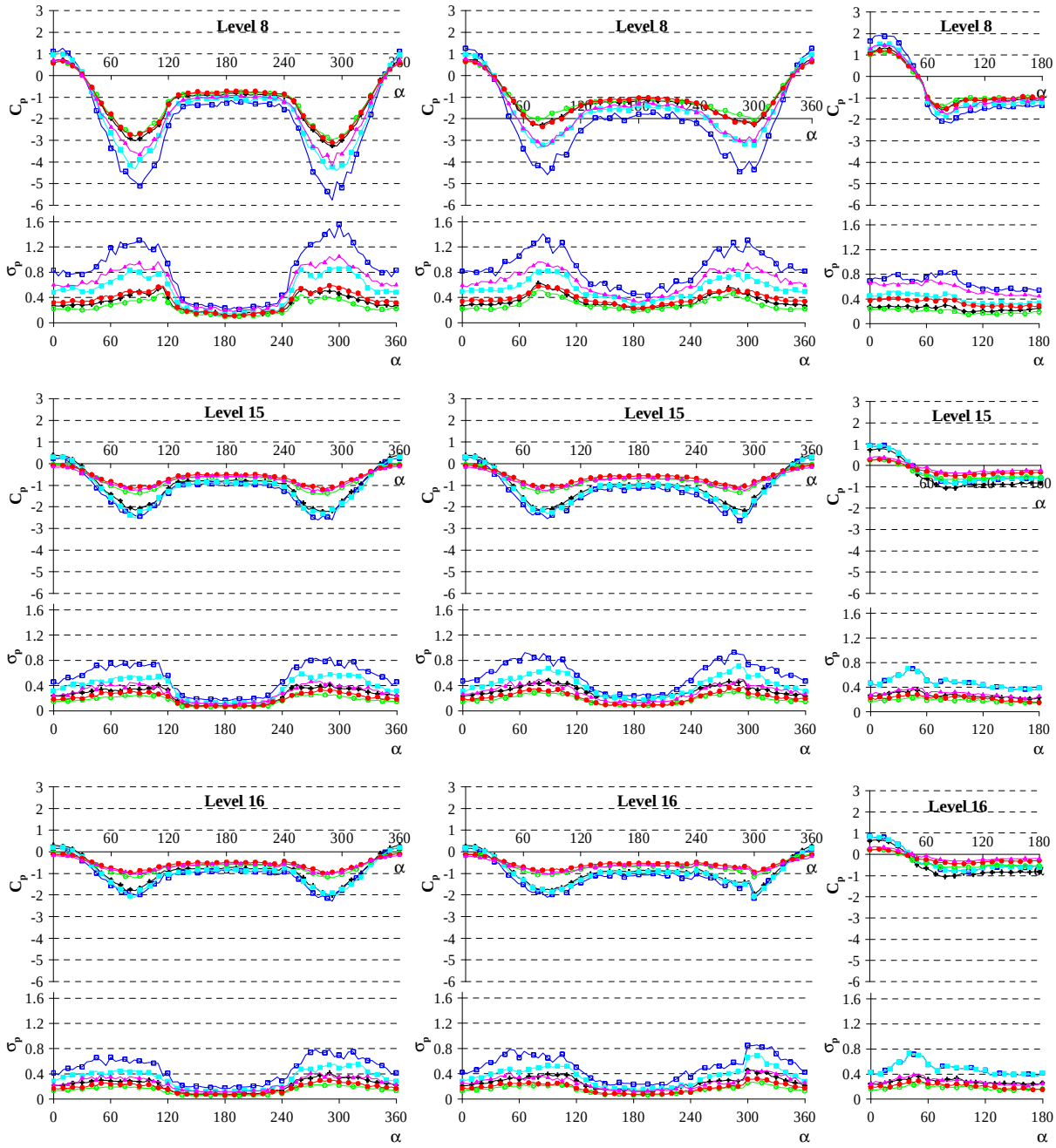

Figure 6. Circumferential distributions of C_p and σ_p for various models against wind structure.

Vertical distribution

Vertical distributions of C_p are presented in various locations around circumference: at the angle 0º where pressure is maximal, at the angle about 30º where pressure changes to suction, at the angle about 75º where the maximal suction is, at the angle 180º where at leeward side the minimal suction is.

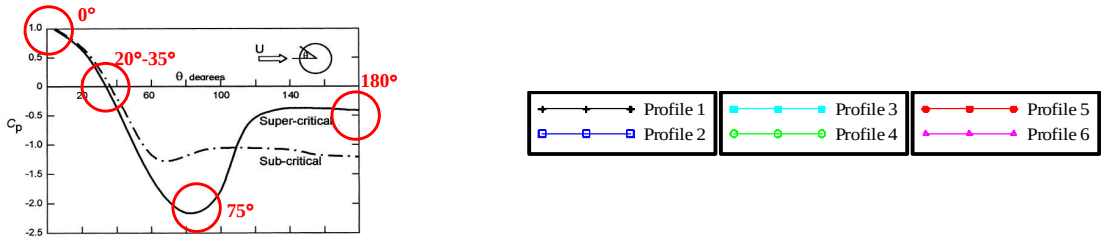

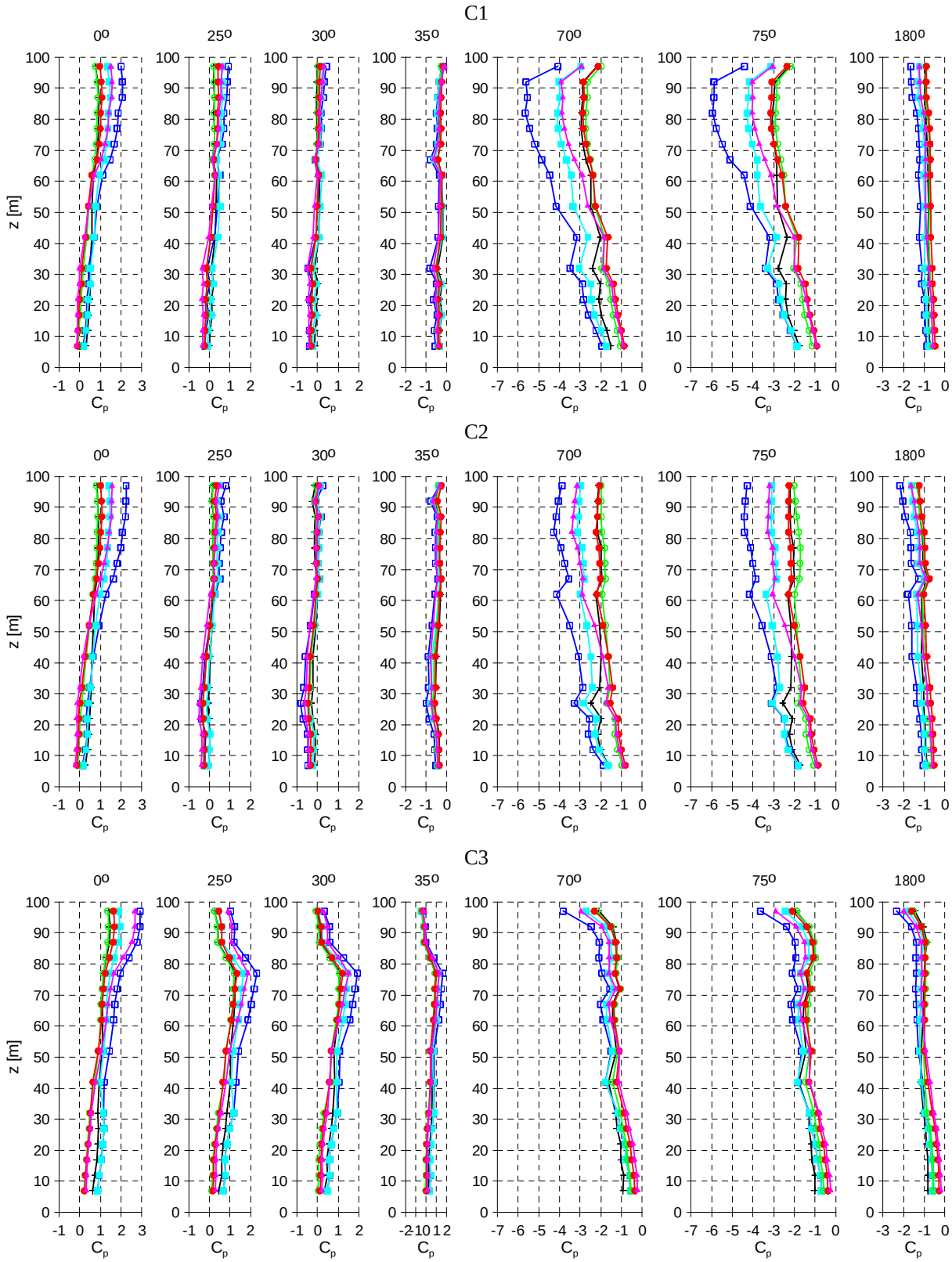

Figure 7. Vertical distributions of C_p for various models against wind structure.

Analyzing the pressure coefficient distributions it can be noticed that for each model they are similar, but there are significant differences in values. Large differences also exist in the values of C_p for each model separately, depending on the wind structure.

Mean pressure coefficient for angle 0° grows at higher levels and reaches peak value at 80-90% of the models height. Differences between profiles are bigger at higher levels, whereas at

lower levels values of C_p are much closer. It is caused by larger differences in wind speeds at higher levels.

Variations of standard deviation are bigger at higher levels and getting smaller at lower levels of models. In general the relative differences in values of standard deviation are much bigger than the ones observed for the mean pressure coefficient.

Mean wind pressure coefficient changes its sign at levels near the base in case of large models C1 and C2 and there is suction round the whole circumference (profiles 4, 5, 6). This is the result of the turbulence increase for these cases of flow. Such a phenomenon was not observed for the model C3 what may be caused by a larger slenderness of this model.

The sequence of plots of the mean wind pressure coefficient as well as standard deviation is similar for each of the models. The highest pressure is for the case of the approaching flow 2, slightly lower for 6 and 3 (similar), then 5, and the smallest for 4 and 1 (similar) at higher levels of the model. At lower levels the relative values of pressure coefficient increase in case of profile 3, and decrease in cases 5 and 6. At levels at the base the highest pressure appears for profiles 1, 2, 3, but the relative differences are much smaller.

The way C_p values change along the model height is in good accordance with changes of wind speed obtained in wind profiles graphs.

The standard deviation is the highest in case 2 then 3, 6, 1, 5, and the lowest in case 4, and this sequence is in principle the same.

Values of mean pressure coefficient and reduced standard deviation at leeward side (for angle about 180°) are slightly increasing with the height.

The highest suction coefficient is for profile 2 then 6 and 3 (similar) and then 5, 4, 1 (similar), so, the sequence is the same like for the angle 0°. At levels near the base there is significant relative increase of suction for profile 1, and decrease for 4 and 6.

Extreme values of suction appear at the angle of about 75° and also increase with the height.

The sequence is the same for angles 0° and 180°. In case of profile 1 the suction is relatively to other cases higher at the base.

The point where coefficient changes its sign in the top regions is more or less constant and located at about 30°. This angle decreases at lower levels and close to the ground there is only suction.

Analyzing the vertical distributions of pressure coefficient it can be noticed that the smallest changes of values in any position around circumference are in case of profile 1, while the highest in case 6.

Settings of the turbulizing elements were chosen to give different values of exponents α in functions describing the mean wind speed profile. Exponent values are approximately equal to 0.2, 0.3, 0.4, and 0.5. In addition, power spectral density functions were assumed to give different values of their extremes, and in case of flow 2 and 3 as well as 5 and 6, for which the exponent α takes respectively similar values, were significantly different.

Comparison of the spectra in range from 0 to 2 Hz (for height of 71 cm) to the pressure coefficients shows that the order of these graphs (PSD and C_p) for the analyzed wind profiles is the same. Taking into account power spectral density functions at other levels (51 cm and 31 cm) such remark cannot be formulated. The influence of power spectral density on C_p distribution is ambiguous and needs to be investigated in details.

CONCLUSIONS

Wind structure affects the distributions of mean wind pressure coefficient as well as its standard deviation. The patterns of C_p and σ_p are similar in all cases of the approaching flow.

There are significant differences in values of analyzed parameters between various flows. Differences appear also along the height of each model within the single profile.

The dependence on the mean wind profile is clear – values of C_p at consecutive levels vary with accordance with variations of wind speed in different profiles. The distribution of spectrum function has also the influence on the pressure values and their standard deviations but it is not unique. It seems that the values of pressures coefficients are larger for the flows described by the functions of the normalized spectrum characterized by higher peak values.

An interesting observation is that only suction appears at bottom levels all around the circumference in cases of the approaching wind with high turbulence.

The flow around the free end of models is evidently affected by 3D character of the flow.

REFERENCES

Adaramola M. S., Akinlade O. G., Sumner D., Bergstrom D. J., Schenstead A. J. (2006): *Turbulent wake of a finite circular cylinder of small aspect ratio*, Journal of Fluids and Structures, Vol. 22, pp. 919–928

Adaramola M. S., Sumner D., Bergstrom D. J., (2010): *Effect of velocity ratio on the streamwise vortex structures in the wake of a stack*, Journal of Fluids and Structures, Vol. 26, pp. 1–18

Cao S., Ozono S., Hirano K., Tamura Y. (2007): *Vortex shedding and aerodynamic forces on a circular cylinder in linear shear flow at subcritical Reynolds number*, Journal of Fluids and Structures, Vol. 23, pp. 703–714

Cao S., Tamura Y. (2008): *Flow around a circular cylinder in linear shear flows at subcritical Reynolds number*, Journal of Wind Engineering and Industrial Aerodynamics, Vol. 96, pp. 1961–1973

Capone D. E., Lauchle G. C. (2000): *Modeling the unsteady lift and drag on a finite-length circular cylinder in cross-flow*, Journal of Fluids and Structures, Vol. 14, pp. 799-817

Capone D. E., Lauchle G. C. (2002): *Modelling the unsteady axial forces on a finite-length circular cylinder in cross-flow*, Journal of Fluids and Structures, Vol. 16(5), pp. 667-683

Garg R. K., Niemann H. J. (1995): *On three dimensionality of fluctuating aerodynamic forces on circular cylindrical structures*, Proceedings of the 9th International Conference on Wind Engineering, New Delhi, India, pp. 129-140

Garg R. K., Niemann H. J., Kasperski M., Chaundhry (1999): *Aspect ratio effects on the aerodynamics of short circular cylindrical structures*, Proceedings of the 10th International Conference on Wind Engineering, Copenhagen, Denmark, pp. 1649-1655

Iungo G. V., Pii L. M., Buresti G. (2012): *Experimental investigation on the aerodynamic loads and wake flow features of a low aspect-ratio circular cylinder*, Journal of Fluids and Structures, Vol. 28, pp. 279–291

Lee S. J., Park C. W. (1999): *Aspect ratio effect on the near wake of a free-ended circular cylinder in a cross-flow*, Proceedings of the 10th International Conference on Wind Engineering, Copenhagen, Denmark, pp. 1687-1692

Luo S. C., Gan T. L., Chew Y. T. (1996): *Uniform flow past one (or two in tandem) finite length circular cylinder(s)*, Journal of Wind Engineering and Industrial Aerodynamics, Vol. 59, pp. 69-93

Park C. W., Lee S. J. (2000): *Free-end effects on the near wake flow structure behind a finite circular cylinder*, Journal of Wind Engineering and Industrial Aerodynamics, Vol. 88, pp. 231–246

Park C. W., Lee S. J. (2002): *Flow structure around a finite circular cylinder embedded in various atmospheric boundary layers*, Fluid Dynamic Research, Vol. 30 (4), pp. 197–215

Park C. W., Lee S. J. (2004): *Effects of free-end corner shape on flow structure around a finite cylinder*, Journal of Fluids and Structures, Vol. 19, pp. 141–158

Sumner D., Heseltine J. L. (2004): *Tip vortex structure for a circular cylinder wit free ends*, Proceedings of the 5th Colloquium on Bluff Body Aerodynamics & Applications, p. 423-426

Sumner D., Heseltine J. L., (2008): *Tip vortex structure for a circular cylinder with a free end*, Journal of Wind Engineering and Industrial Aerodynamics, Vol. 96, pp. 1185–1196

Sumner D., Heseltine J. L., Dansereau O. J. P. (2004): *Wake structure of a finite circular cylinder of small aspect ratio*, Experiments in Fluids, Vol. 37, pp. 720-730

Uematsu Y., Yamada M. (1995): *Effects of aspect ratio and surface roughness on the time-averaged aerodynamic forces on cantilevered circular cylinders at high Reynolds numbers*. Journal of Wind Engineering and Industrial Aerodynamics, Vol. 54/55, pp. 301-312

Uematsu Y., Yamada M. (1995): *Fluctuating wind pressures on buildings and structures of circular cross-section at high Reynolds numbers*. Proceedings of the 9th International Conference on Wind Engineering, New Delhi, India. pp. 129-130